Pure Appl. Chem., Vol. 82, No. 4, pp. 991–999, 2010.
doi:10.1351/PAC-CON-09-10-02

Effect of molecular clips and tweezers on enzymatic reactions by binding coenzymes and basic amino acids*

Frank-Gerrit Klärner[1,‡], Thomas Schrader[1], Jolanta Polkowska[1], Frank Bastkowski[1], Peter Talbiersky[1], Mireia Campañá Kuchenbrandt[1], Torsten Schaller[1], Herbert de Groot[2], and Michael Kirsch[2]

[1]Institute for Organic Chemistry, University of Duisburg-Essen, Universitätsstrasse 7, 45117 Essen, Germany; [2]Institute for Physiological Chemistry, Universitätsklinikum Essen, Hufelandstrasse 55, 45122 Essen, Germany

Abstract: The tetramethylene-bridged molecular tweezers bearing lithium methanephosphonate or dilithium phosphate substituents in the central benzene or naphthalene spacer-unit and the dimethylene-bridged clips containing naphthalene or anthracene sidewalls substituted by lithium methanephosphonate, dilithium phosphate, or sodium sulfate groups in the central benzene spacer-unit are water-soluble. The molecular clips having planar naphthalene sidewalls bind flat aromatic guest molecules preferentially, for example, the nicotinamide ring and/or the adenine-unit in the nucleotides NAD(P)$^+$, NMN, or AMP, whereas the benzene-spaced molecular tweezers with their bent sidewalls form stable host–guest complexes with the aliphatic side chains of basic amino acids such as lysine and argenine. The phosphonate-substituted tweezer and the clips having an extended central naphthalene spacer-unit or extended anthracene and benzo[k]fluoranthene sidewalls, respectively, form highly stable self-assembled dimers in aqueous solution, evidently due to non-classical hydrophobic interactions. The phosphate-substituted molecular clip containing naphthalene sidewalls inhibits the enzymatic, ADH-catalyzed ethanol oxidation by binding the cofactor NAD$^+$ in a competitive reaction. Surprisingly, tweezer-bearing phosphate substituents in the central benzene spacer-unit are more efficient inhibitors for the ethanol oxidation than the correspondingly substituted naphthalene clip, even though the tweezer does not bind the cofactor NAD$^+$ within the limits of detection. The phosphate-substituted naphthalene clip is, however, a highly efficient inhibitor of the enzymatic oxidation of glucose-6-phosphate (G6P) with NADP$^+$ catalyzed by glucose-6-phosphate dehydrogenase (G6PD), whereas the phosphonate-substituted clip only functions as an inhibitor by forming a complex with the cofactor. Detailed kinetic, thermodynamic, and computational modeling studies provide insight into the mechanism of these novel enzyme inhibition reactions.

Keywords: alcohol dehydrogenase; enzyme inhibitors; glucose-6-phosphate dehydrogenase; host–guest complexes; molecular clips; molecular tweezers.

Pure Appl. Chem.* **82, 757–1063 (2010). An issue of reviews and research papers based on lectures presented at the 13th International Symposium on Novel Aromatic Compounds (ISNA-13), 19–24 July 2009, Luxembourg City, Luxembourg on the theme of aromaticity.
‡Corresponding author

INTRODUCTION

Aromatic interactions play an important role in the processes of molecular recognition and self-assembly [1]. We started our own investigation of tweezers and clips with the simple question of whether multiple arene–arene interactions lead to synergetic effects as it has been observed for multiple hydrogen bonding. To answer this question, the parent and the diacetoxy-substituted tetramethylene-bridged tweezers **1,2** and the tri- and dimethylene-bridged clips **3–6** (R = H, OAc, Fig. 1) were synthesized [2]. These molecules are well preorganized because of their belt-type structures. Indeed, they form stable host–guest complexes, e.g., in chloroform solution, by multiple arene–arene interactions. Generally, the complexes of the tweezers **1,2** having five aromatic binding sites are more stable than those of the clips **3–6** having only four or three aromatic binding sites. Surprisingly, all these host molecules only bind electron-poor cationic or neutral aromatic and aliphatic guest molecules inside their cavities. No complex formation has been detected with electron-rich systems. This finding has been explained with the electrostatic potential surfaces (EPSs) which were calculated to be highly negative inside the tweezer or clip cavity and hence complementary to the positive EPS of the guest molecules which are bound by these host molecules [3]. In the following we discuss the properties of water-soluble systems and their influence on enzymatic reactions.

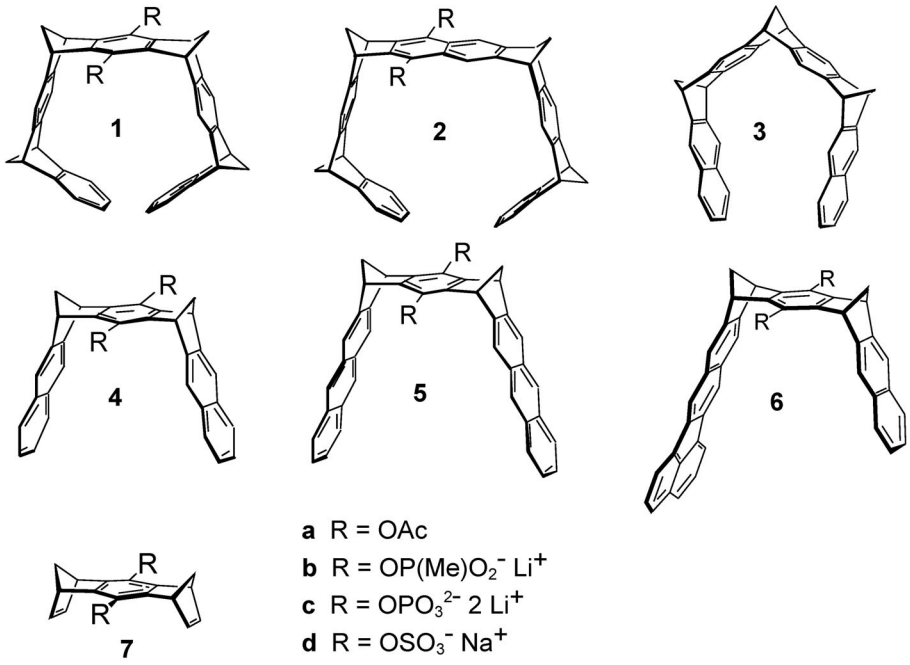

Fig. 1 Structures of the molecular tweezers **1,2**, clips **3–6**, and bridges **7**.

RESULTS AND DISCUSSION

Molecular tweezers and clips bearing phosphonate, phosphate, or sulfate substituents in the central benzene or naphthalene bridges are water-soluble. The derivatives **1b**, **1c**, **2b**, **4b–d**, **5b**, and **5d** were already reported in the literature [4–9]. The hitherto unknown phosphonate-substituted clip **6b** (having one extended benzo[*k*]fluoranthene and one naphthalene sidewall) was synthesized from **6a** (R = OAc) in three steps [10] analogously to the corresponding clips **4b** and **5b** [5,7] (for detailed description, see Supplementary Information).

The naphthalene-bridged tweezer **2b** and the clips **5b,d** and **6b** having expanded anthracene or benzo[*k*]fluoranthene sidewalls form highly stable self-assembled dimers in water, whereas dimers of the benzene-bridged tweezers **1b,c** and naphthalene clips **4b,c,d** are weak. The structures of the dimers $(\mathbf{2b})_2$ and $(\mathbf{5b})_2$ shown in Fig. 2 were assigned by comparison of their experimental chemical ^{1}H NMR shifts with those calculated by quantum-chemical ab initio methods [7]. The ^{1}H NMR shift data of dimer $(\mathbf{6b})_2$ suggest an intertwined structure comparable to that of $(\mathbf{5b})_2$ (see Supplementary Information, Fig. S4). All these systems exist as monomers in pure methanol. The negative values of the enthalpy and entropy of dimerization (Table 1) indicate that nonclassical hydrophobic interactions [1] are responsible for the observed dimer formation in water.

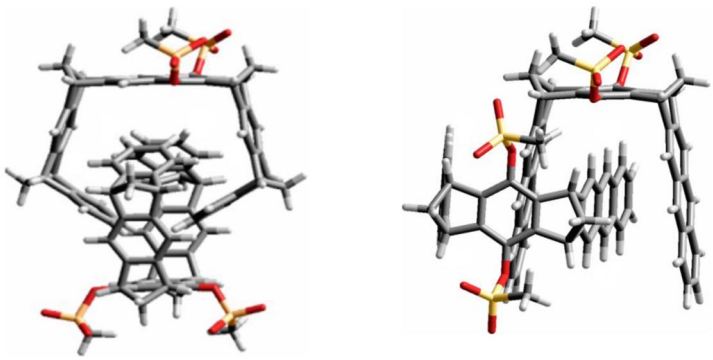

$(\mathbf{2b})_2$ $(\mathbf{5b})_2$

Fig. 2 Structures of the dimers of phosphonate-substituted naphthalene tweezer $(\mathbf{2b})_2$ and anthracene clip $(\mathbf{5b})_2$ calculated by force field (MacroModel 6.5, Amber*/H_2O, Monte Carlo conformer search, 5000 structures).

Table 1 The thermodynamic parameters, log K_{Dim} [M^{-1}], ΔG [kcal mol^{-1}], ΔH [kcal mol^{-1}], and $T\,\Delta S$ [kcal mol^{-1}] determined for the self-assembled dimerization of the molecular tweezers and clips at 298 K in aqueous solution by ^{1}H NMR spectroscopy at variable temperatures [7,8].

Reaction	log K_{Dim}	ΔG	ΔH	$T\,\Delta S$
2 **1c** ⇆ $(\mathbf{1c})_2$[a]	1.7			
2 **2b** ⇆ $(\mathbf{2b})_2$	**6.4**	**–8.7**	**–20.9**	**–12.2**
2 **4c** ⇆ $(\mathbf{4c})_2$[a]	2.1			
2 **4d** ⇆ $(\mathbf{4d})_2$	2.5			
2 **5b** ⇆ $(\mathbf{5b})_2$	**5.2**	**–7.1**	**–13.8**	**–6.7**
2 **5b** ⇆ $(\mathbf{5b})_2$[a]	**5.2**	**–7.5**	**–8.9**	**–1.4**
2 **5d** ⇆ $(\mathbf{5d})_2$	**5.3**	**–7.2**	**–12.4**	**–5.2**
2 **6b** ⇆ $(\mathbf{6b})_2$	**6.0**	**–8.1**	**–15.2**	**–7.1**

[a]In buffered aqueous solution at pH = 7.2 [11].

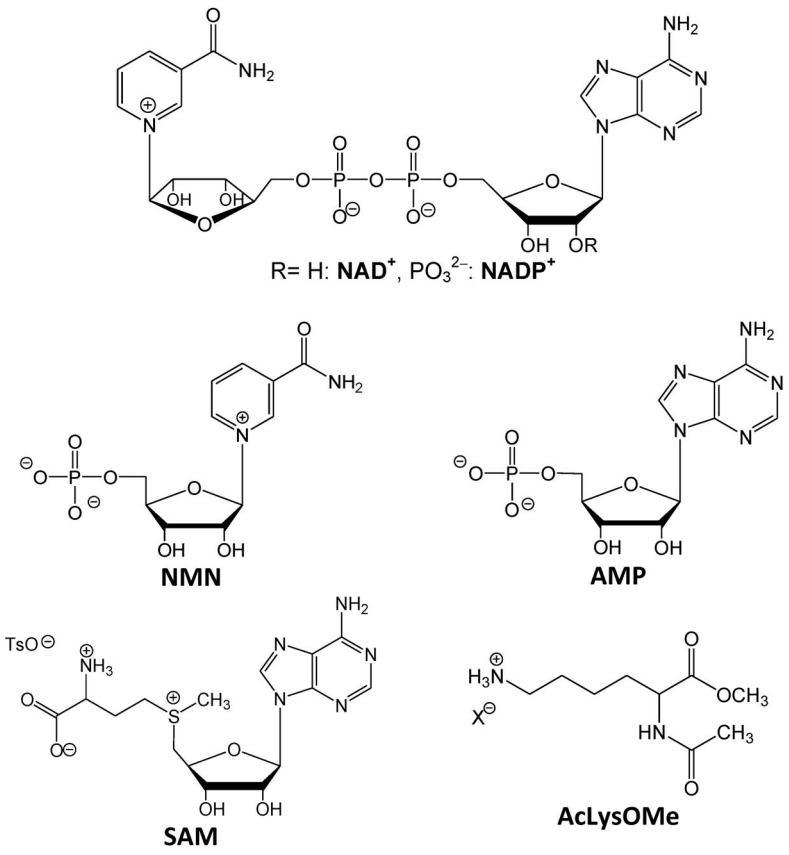

Fig. 3 Structures of the guest molecules which form host–guest complexes with molecular tweezers and clips in buffered aqueous solution at pH = 7.2.

Nicotinamide adenine dinucleotide NAD^+ and nicotinamide adenine dinucleotide phosphate $NADP^+$ form stable host–guest complexes with the phosphonate- and phosphate-substituted clips **4b** and **4c** in buffered aqueous solution at neutral pH. The binding constants were determined by spectrofluorimetric and ^{1}H NMR titration experiments to be log K_a [M^{-1}] = 3.7 (NAD^+ · **4b**), 3.9 (NAD^+ · **4c**), 3.7 ($NADP^+$ · **4b**), and 3.7 ($NADP^+$ · **4c**) [12,13]. The structures of the host–guest complexes of the clips **4b** and **4c** with NAD^+ were elucidated by quantum-chemical ^{1}H NMR shift calculations [12]. For example, the complexation-induced ^{1}H NMR shifts, $\Delta\delta_{max}$, calculated for the structure shown in Fig. 4 (left) agree well with the experimental data of complex NAD^+ · **4b**, indicating that the active site of NAD^+, the nicotinamide ring, is preferentially located inside the clip cavity. Similar large $\Delta\delta_{max}$ values of the guest protons were found for the related complexes between $NAD(P)^+$ and clips **4b,c**. The mononucleotides NMN and AMP, the fragments of NAD^+, both form complexes with the clips **4b,c** of smaller stability (log K_a [M^{-1}] = 2.7 (NMN · **4b**), 3.1 (NMN · **4c**), 3.0 (AMP · **4b**), and 2.8 (AMP · **4c**). They display, however, large $\Delta\delta_{max}$ values of the guest protons attached to the nicotinamide ring in NMN and adenosine unit in AMP. These $\Delta\delta_{max}$ values are of similar size to those found for corresponding protons in the complexes between $NAD(P)^+$ and clips **4b,c**. These findings suggest the incorporation of the adenosine unit inside the clip cavity in the $NAD(P)^+$ complexes, too, presumably to a minor extent. These structures exist in a rapid equilibrium with the complex structures including the nicotinamide ring. The clips **4b,c** also bind *S*-adenosylmethionine {log K_a [M^{-1}] = 3.1 (SAM · **4b**) and 3.7 (SAM · **4c**)} [6]. The large complexation-induced ^{1}H NMR shifts, $\Delta\delta_{max}$, found for the methylene

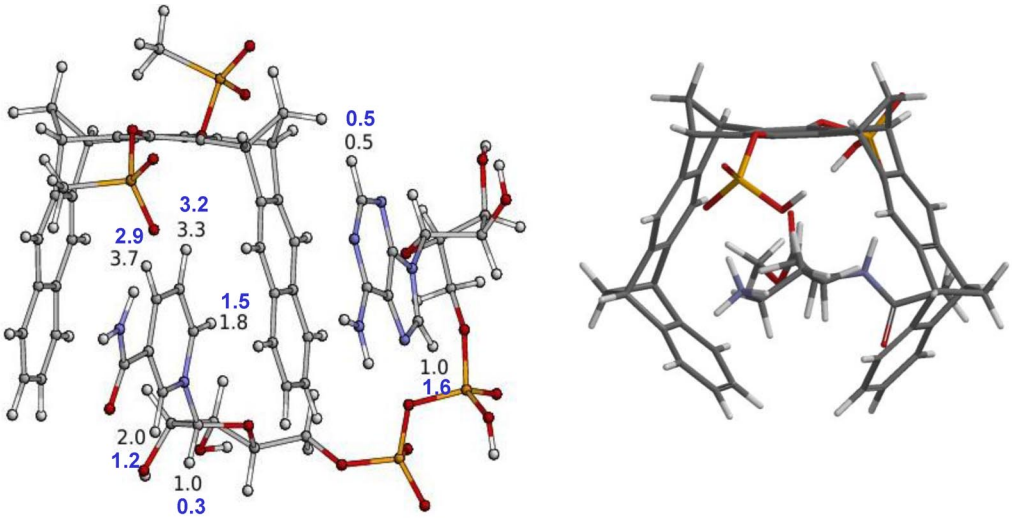

Fig. 4 Structures of the host–guest complexes calculated by force field (MacroModel 8.1, Monte Carlo conformer search, 5000 structures, AMBER*/H_2O), left: NAD^+ · **4** [R = $OP(Me)O_2$], comparison of the experimental complexation-induced ^1H NMR shifts, $\delta\Delta_{max}$, of the NAD^+ guest protons (in blue obtained by NMR titration) with those (in black computed by quantum-chemical methods at the GIAO-HF/SVP level) [12], right: AcLysOMe · **1** (R = $OP(OH)O_2^-$).

and methyl protons of the $[CH_2S^+(CH_3)CH_2]$ group suggest that this side chain of SAM is preferentially positioned inside the clip cavity. The benzene tweezers **1b,c** do not bind NAD^+ within the limits of NMR detection. They bind, however, basic amino acids such as lysine and arginine. The complexes of the phosphate-substituted tweezer **1c** are substantially more stable than those of the phosphonate tweezer **1b** (e.g., log K_a [M^{-1}] = 4.8 (AcLysOMe · **1c**) and 3.6 (AcLysOMe · **1b**) [4,13]. This finding is in contrast to that of the host–guest complexes of the phosphonate- and phosphate-substituted clips **4b,c** which only showed small differences in their stability. The large $\Delta\delta_{max}$ value observed for methylene protons attached to the ammonium function of AcLysOMe indicates that the lysine aliphatic side chain is included inside the tweezer cavity as indicated by the complex structure calculated by a Monte Carlo simulation (Fig. 4, right).

The phosphate clip **4c** inhibits the enzymatic oxidation of ethanol with NAD^+ catalyzed by alcohol dehydrogenase (ADH) with IC_{50} = 1500 μM and the ratio $IC_{50}/[NAD^+]$ = 0.8 (IC_{50} – inhibitor concentration to block 50 % of the enzyme reaction) [13]. The kinetic analysis suggests that the concentration of the cofactor, NAD^+, is depleted by binding to clip **4c**. The result that a substoichiometric amount of the phosphate tweezer **1c** readily inhibits this reaction (IC_{50} = 180 μM, $IC_{50}/[NAD^+]$ = 0.09) is surprising. Since the tweezer does not bind to NAD^+, we assume that the tweezer is bound to the lysine moieties of the enzyme close to the active site and, hence, blocks the binding of the cofactor to this site. This assumption is strongly supported by the finding that the inhibited reaction can be switched on by addition of an external lysine derivative and again switched off by further addition of the tweezer (Fig. 5).

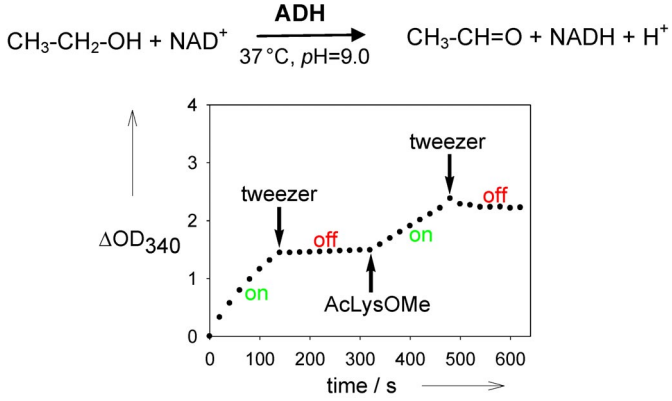

Fig. 5 Alternating addition of tweezer **1c** and AcLysOMe turns enzyme activity off and on.

A remarkable example is the effect of the clips **4b,c** on the enzymatic oxidation of glucose-6-phosphate (G6P) with $NADP^+$ catalyzed by glucose-6-phosphate dehydrogenase (G6PD) (Scheme 1) [14]. This reaction is the first step in the pentose-phosphate pathway.

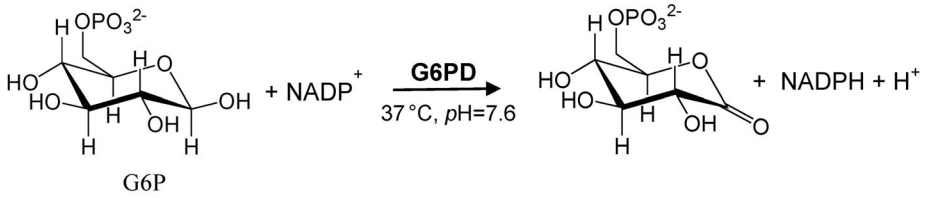

G6P

Scheme 1 Oxidation of G6P with $NADP^+$ catalyzed by G6PD.

The phosphonate-substituted clip **4b** (needed in stoichiometic amounts) inhibits the enzymatic G6P oxidation, apparently, by binding the cofactor $NADP^+$, whereas the phosphate-substituted clip **4c** is a much more efficient inhibitor which is only required in substoichiometric amounts (Table 2). Evidently, the phosphate groups provide a substantial contribution to the efficiency of these inhibitors. This is also demonstrated by the study of the bridges **7b,c**. Only the phosphate-substituted bridge **7c** shows a significant inhibition which is, however, smaller than that of clip **4c**. This finding indicates that the clip sidewalls are also important for the inhibition increasing the inhibitor potency of these systems.

Table 2 Inhibition of the enzymatic oxidation of G6P (2 mM) with $NADP^+$ (200 μM) catalyzed by G6PD with the phosphonate- and phosphate-substituted molecular clips **4b,c** and bridges **7b,c** at 37 °C in aqueous buffered solution at pH = 7.6.

Inhibitor	IC_{50} [μM]	IC_{50}/[$NADP^+$]
Clip **4b** [R = $OP(Me)O_2^-$ Li^+]	350	1.8
Bridge **7b** [R = $OP(Me)O_2^-$ Li^+]	>500	>2.5
Clip **4c** (R = OPO_3^{2-} 2 Li^+)	**7**	**0.03**
Bridge **7c** (R = OPO_3^{2-} 2 Li^+)	53	0.27

Clip **4c** produces a very rare Lineweaver–Burk plot in which the native and inhibition curves intersect in the positive *x*,*y* quadrant in sharp contrast to clip **4b** which shows the intersection of these two curves on *y*-axis indicative for a competitive inhibition (Fig. 6, left). According to theoretical studies by Dixon and Webb and by Whiteley [15], the unusual slope found for clip **4c** is characteristic of partial uncompetitive inhibition. From detailed kinetic and thermodynamic studies [14] we propose the following mechanism for the inhibition of the enzymatic G6P oxidation by the phosphate clip **4c**, according to the X-ray structure, the enzyme has two binding sites, the so-called Rossman fold and the substrate site. The binding of substrate and/or cofactor to the substrate site seems to stabilize the active enzyme structure and prevents its denaturation. We measured the Gibbs enthalpies for the binding of cofactor $NADP^+$ and clip **4c** to the enzyme G6PD as well as the binding of clip **4c** or cofactor to the corresponding binary complexes by a combination of isothermal titration calorimetry (ITC) and fluorometric titration experiments (Fig. 6, right). Both pathways lead to a stable ternary complex consisting of the enzyme, one clip molecule, and one molecule of $NADP^+$. The substrate binding site is additionally blocked by one clip molecule. We assume that this complex is responsible for the efficient blocking of the enzymatic reaction by clip **4c**. This assumption is supported by molecular dynamics (MD) calculations. The enzyme was calculated to form a stable ternary complex, in which the adenine unit of $NADP^+$ is bound inside the clip cavity (Fig. 7, left). A second binary enzyme complex was calculated with clip **4c** occupying the substrate binding site (Fig. 7, right).

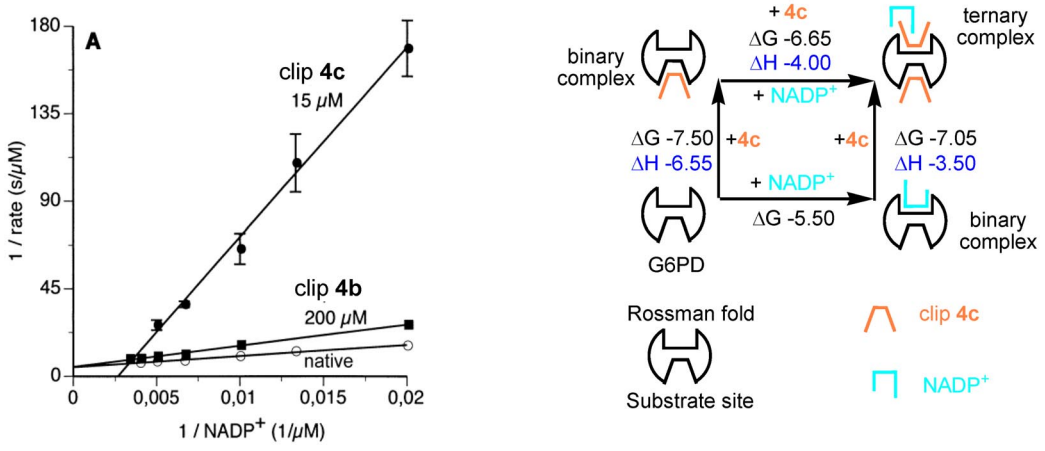

Fig. 6 Left: Enzyme kinetics of reaction G6P with $NADP^+$ catalyzed by G6PD, with clip **4b** conventional competitive and with clip **4c** partial uncompetitive cofactor inhibition. Right: Thermodynamic figure for successive complex formation between G6PD, clip **4c** and $NADP^+$ (both in excess), explaining the unusual and highly efficient inhibition kinetics; ΔH, ΔG in kcal/mol.

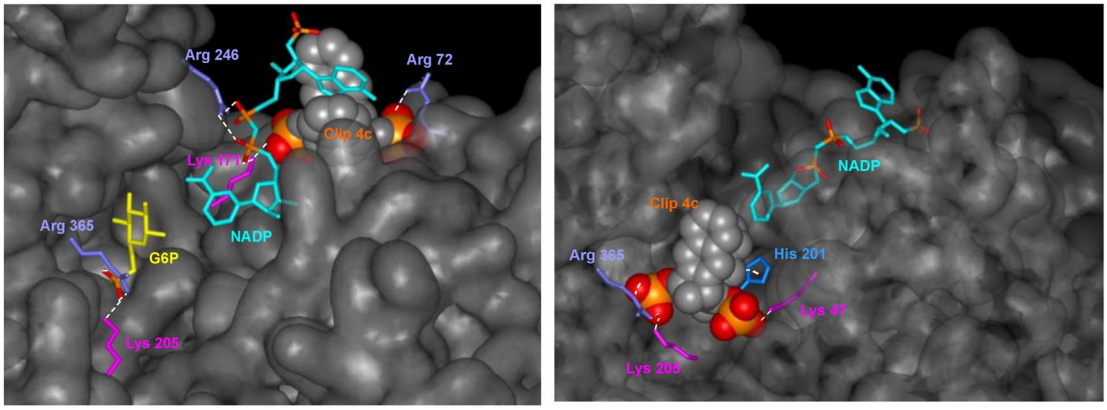

Fig. 7 MD simulations of ternary and binary complex illustrating the two inhibition modes of G6PD by clip **4c**: left: virtual cofactor replacement by clip **4c** with subsequent redocking of $NADP^+$ inside the clip; right: calculated enzyme complex with clip **4c** occupying the substrate binding site.

CONCLUSIONS

The molecular tweezers **1,2** and clips **4–6** bearing phosphonate, phosphate, and sulfate substituents in the central spacer unit are water-soluble. In buffered aqueous solution, the molecular clips **4b,c,d** containing planar naphthalene sidewalls bind flat aromatic guest molecules preferentially, for example, the nicotinamide ring of $NAD(P)^+$ and NMN but also the adenine unit in AMP, whereas the molecular tweezers **1b,c** with their bent sidewalls form stable complexes with the aliphatic side chains of basic amino acids such as lysine and arginine. The circumstances are more complicated in pure water where NAD^+ reacts as a weak acid forming a self-aggregate which is only cleaved in excess of clip **4b**. Mixtures of clip and NAD^+ (1:1) in water lead to less well defined associates of the clip presumably to the outside of the NAD^+ aggregate. The complex between SAM and clip **4b** precipitates from water, whereas it is soluble in buffered solution. The tweezer **2b** and the clips **5b,d** and **6b** having an extended central naphthalene spacer unit or extended anthracene and benzo[*k*]fluoranthene sidewalls form highly stable self-assembled dimers in aqueous as well as in buffered aqueous solution, evidently due to non-classical hydrophobic interactions. The molecular clip **4c** inhibits the enzymatic, ADH-catalyzed ethanol oxidation by binding the cofactor NAD^+ in a competitive reaction. Surprisingly, tweezer **1c** is a more efficient inhibitor for the ethanol oxidation than clip **4c**, even though **1c** does not bind the cofactor NAD^+ within the limits of detection. Alternating addition of tweezer **1c** and AcLysOMe turns enzyme activity off and on. This finding allows the concluion that tweezer **1c** binds to lysine moieties of the enzyme which are close to the active site and, hence, blocks the enzyme. The phosphate-substituted clip **4c** is, however, a highly efficient inhibitor of the enzymatic oxidation of G6P with $NADP^+$ catalyzed by G6PD, whereas the phosphonate-substituted clip **4b** only functions as a competitive inhibitor by binding the cofactor. Detailed kinetic, thermodynamic, and computational modeling studies allow the conclusion, that the high efficiency of clip **4c** as inhibitor for this reaction is the result of the formation of two stable complexes: One binary complex at the substrate site and one ternary complex consisting of enzyme, clip, and cofactor which blocks the active site of the enzyme. The comparison of the properties of the phosphate- and phosphonate-substituted inhibitors **4c/7c** and **4b/7b** shows that the phosphate groups substantially contribute to efficacy of these systems as inhibitors.

SUPPLEMENTARY INFORMATION

Supplementary information is available online (doi:10.1351/PAC-CON-09-10-02).

ACKNOWLEDGMENTS

This work was supported by the Deutsche Forschungsgemeinschaft. F.-G. K. thanks the colleagues, postdocs, and students cited in the references [2–14] for the highly stimulating and fine collaboration.

REFERENCES

1. Review: E. A. Meyer, R. K. Castellano, F. Diederich. *Angew. Chem., Int. Ed*. **42**, 1210 (2003).
2. Reviews: (a) F.-G. Klärner, B. Kahlert. *Acc. Chem. Res.* **36**, 919 (2003); (b) F.-G. Klärner, M. Campana Kuchenbrandt. "Synthesis of molecular tweezers and clips by the use of a molecular Lego set and their supramolecular functions", in *Strategies and Tactics in Organic Synthesis*, Vol. 7, Chap. 4, pp. 99–153, M. Harmata (Ed.), Academic Press-Elsevier, Amsterdam (2008).
3. (a) M. Kamieth, F.-G. Klärner, F. Diederich. *Angew. Chem., Int. Ed.* **37**, 3303 (1998); (b) F.-G. Klärner, J. Panitzky, D. Preda, L. T. Scott. *J. Mol. Model.* **6**, 318 (2000); most recently, the substituent effect on the electrostatic potential surface of aromatic systems was explained to be a through-space interaction largely; (c) S. E. Wheeler, K. N. Houk. *J. Chem. Theory Comput.* **5**, 2301 (2009) doi:10.1021/ct900344g.
4. M. Fokkens, T. Schrader, F.-G. Klärner. *J. Am. Chem. Soc*. **127**, 14415 (2005).
5. M. Fokkens, C. Jasper, T. Schrader, F. Koziol, C. Ochsenfeld, J. Polkowska, M. Lobert, B. Kahlert, F.-G. Klärner. *Chem.–Eur. J.* **11**, 477 (2005).
6. T. Schrader, M. Fokkens, F.-G. Klärner, J. Polkowska, F. Bastkowski. *J. Org. Chem*. **70**, 10227 (2005).
7. F.-G. Klärner, B. Kahlert, A. Nellesen, J. Zienau, C. Ochsenfeld, T. Schrader. *J. Am. Chem. Soc.* **128**, 4831 (2006).
8. B. Branchi, P. Ceroni, V. Balzani, M. C. Cartagena, F.-G. Klärner, T. Schrader, F. Vögtle. *New J. Chem*. **33**, 397 (2009).
9. B. Branchi, V. Balzani, P. Ceroni, M. Campana Kuchenbrandt, F.-G. Klärner, D. Bläser, R. Boese. *J. Org. Chem.* **73**, 5839 (2008).
10. The preparation of molecular clip **6b** and the determination of the thermodynamic parameters listed in Table 1 for the formation of its self-assembled dimer $(\mathbf{6b})_2$ are described by M. Campana Kuchenbrandt, Ph.D. thesis, University of Duisburg-Essen, 2007, and in the Supplementary Information.
11. C. J. Breitkreuz. Diploma thesis, University of Duisburg-Essen (2006).
12. J. Polkowska, F. Bastkowski, T. Schrader, F.-G. Klärner, J. Zienau, F. Koziol, C. Ochsenfeld. *J. Phys. Org. Chem*. **22**, 779 (2009).
13. P. Talbiersky, F. Bastkowski, F.-G. Klärner, T. Schrader. *J. Am. Chem. Soc*. **130**, 9824 (2008).
14. M. Kirsch, P. Talbiersky, J. Polkowska, F. Bastkowski, T. Schaller, H. de Groot, F.-G. Klärner, T. Schrader. *Angew. Chem., Int. Ed*. **48**, 2886 (2009).
15. (a) M. Dixon, E. C. Webb. *Enzymes*, pp. 343–344, Longman, London (1979); (b) C. G. Whiteley. *Biochem. Educ.* **28**, 144 (2000).

